CYCLIC LOADING TEST OF MAGNETORHEOLOGICAL (MR) DAMPER

Anat RUANGRASSAMEE[1] and Kazuhiko KAWASHIMA[2]

[1]M. of Eng., Graduate Student, Dept. of Civil Eng., Tokyo Institute of Technology
(2-12-1, O-okayama, Meguro-ku, Tokyo 152-8552, Japan)
[2]Dr. of Eng., Professor, Dept. of Civil Eng., Tokyo Institute of Technology
(2-12-1, O-okayama, Meguro-ku, Tokyo 152-8552, Japan)

This study is conducted to investigate the applicability of a magnetorheological (MR) damper in the semi-active control of bridge responses. A series of cyclic loading test was carried out on a MR damper under various loading displacements, loading frequencies, and input current. The damping force of the MR damper was idealized by Bingham model. Two algorithms to change the damping force according to relative displacement or relative velocity were tested. It is found that the commanded damping force can be realized by the MR damper. However, some discrepancies are observed, especially when the damping force is abruptly changed.

Key Words: *magnetorheological damper, variable damper, semi-active control, control algorithm*

1. INTRODUCTION

Under strong ground motion, bridge piers may experience nonlinearity and bridge decks unseat from piers or abutments. Highway bridges are conventionally designed to behave passively during earthquakes. The seismic performance of the bridges is assured for some particular target ground motions. However, earthquake motion is stochastic in its nature. There arises the need to make structural properties more adaptive to responses caused by the unpredictable earthquake motion. To deal with the problem, many researchers have attempted to apply the active and semi-active control systems in the civil engineering structures.

Active control systems have been proved to reduce structural response. However, the response reduction is obtained at the expense of substantial power supply. In addition, the stability requirement of the active control systems limits its applicability. Semi-active control systems come in-between to bridge the gap. Semi-active control systems offer the reliability of passive devices, yet provide the adaptability of active control systems. Because the semi-active control systems are inherently stable and require much less amount of power supply, it is promising to apply the semi-active control systems to civil engineering structures[1].

Semi-active devices have been developed in the recent past decade. Semi-active viscous dampers provide adaptable damping force by adjusting the size of the orifice through which viscous fluid flows when a piston moves in a hydraulic cylinder[2]. Recently, Magetorheological (MR) dampers gain interest from researchers[3), 4), 5)]. MR fluid can operate at temperature from –40 to 150 degree Celsius with only slight variations in yield stress. MR fluid is not sensitive to impurities such as are commonly encountered during manufacturing and usage. MR fluid can be controlled with low power supply (less than 50W).

The study is conducted experimentally to investigate the applicability of a magnetorheological (MR) damper in the semi-active control of bridge responses. A series of cyclic loading test was carried out on a MR damper under various loading displacements, loading frequencies, and input current. Two algorithms to vary the damping force according to relative displacement or relative velocity were tested.

2. CYCLIC LOADING TEST OF MR DAMPER

A RD-1005-5-2 MR damper developed by Lord Corporation is used in this study. The damper is 208 mm long in its extended position and 155 mm long

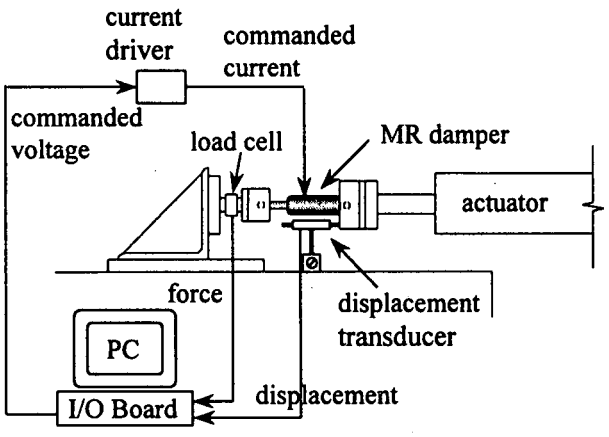

Fig. 1 Test setup of cyclic loading test

in its compressed position. So, the stroke of the damper is about +/- 25 mm. The cylinder is 41 mm in diameter. The damper operates at the current of 0-2 A. The current is supplied to the damper by a Lord RD-3002 current driver. The current driver regulates a 0-2 A output current proportional to a 0-5 V commanded input voltage.

In order to apply a MR damper as a semi-active control device, it is necessary to identify the damping properties of the MR damper. A series of cyclic loading tests is conducted for various loading conditions. Fig. 1 shows the test setup of the cyclic loading test. Reaction force is measured by a load cell with a capacity of 1000 N. The load cell is connected between a reaction frame and a damper. The displacement is measured by a displacement transducer with a capacity of 50 mm. The current to the damper is controlled by a microcomputer. The commanded voltage is generated by an I/O board which is installed in the computer. Then, the current driver supplies a current proportionally to the commanded voltage. A hydraulic actuator with displacement control is used to load the damper.

The damper is loaded with a sinusoidal signal with a fixed frequency and amplitude, while the current to the damper is hold constant. The response of the damper is investigated for a wide range of loading frequencies, loading amplitudes, and current levels. Loading conditions of the cyclic loading tests are summarized in Table 1.

Fig. 2 shows force-displacement curves of the static case for the current levels of 0, 250, and 500 mA. The force-displacement curves are close to a rectangular shape which is typical for a friction damper. The damping forces at maximum velocity are 27, 121, and 306 N for the current levels of 0, 250, and 500 mA, respectively.

Fig. 3 shows response of the MR damper subjected to a 1.5 Hz sinusoid with an amplitude of 20 mm for constant currents of 0, 250, and 500 mA. It is seen that damping force increases as the current

Table 1 Loading conditions of cyclic loading tests

Loading Type	Frequency (Hz)	Amplitude (mm)	Current (mA)
Static	0.05	20	0, 50, 100, 150, 200, 250, 500, 750
Dynamic	0.5, 1.0, 1.5, 2.0, 2.5	5, 10, 15, 20	0, 50, 100, 150, 200, 250, 500, 750

to the damper increases. From Fig. 3 (a), the force-displacement curve of the MR damper is close to that of a friction damper. Focusing on the positive-velocity portion of the force-velocity curve in Fig. 3 (b), the characteristic of a viscous damper that damping force varies linearly with velocity can be observed in the upper branch of the curve. However, the damping force decreases rapidly and smoothly when the velocity is close to zero, causing a hysteretic loop. The change of the damping force at velocity close to zero is not so sudden as the friction damper because of the compressibility of an accumulator in the MR damper and blow-by of fluid between the piston and the cylinder. This can be obviously seen in the force-displacement curve at the maximum displacement. When the direction of loading is reversed, a small movement is required before the damper reaches a certain level of force, causing smooth change of force.

Fig. 4 illustrates comparison of force-displacement curves for various loading frequencies, loading amplitudes, and current levels. The characteristics of the MR damper as mentioned above are also observed for other loading conditions.

3. MODEL OF MR DAMPER

To control the damping force of the MR damper, the model of the MR damper is essential. In this study, the MR damper is modeled by the Bingham model. The Bingham model consists of friction and viscous elements in parallel as illustrated in Fig. 5. The damping force is expressed as

$$f_d = f + cv \tag{1}$$

where f_d is a damping force, f is a friction force, c is a damping coefficient, and v is a velocity.

From the experimental results, maximum loading velocity and damping force at the maximum

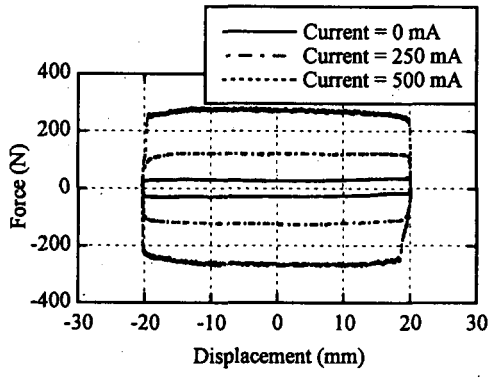

Fig. 2 Force-displacement curves of static cases

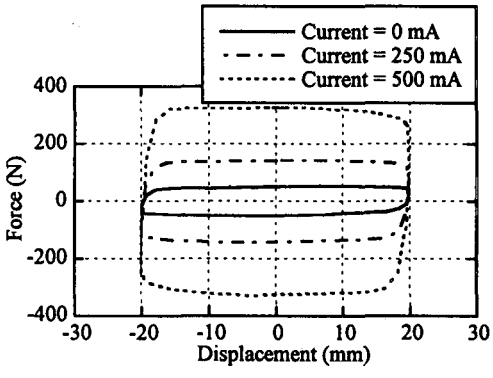

(a) Force-displacement curve

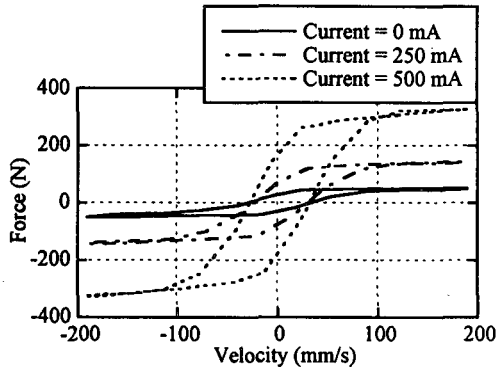

(b) Force-velocity curve

Fig. 3 Response of MR damper subjected to a 1.5 Hz sinusoid with an amplitude of 20 mm

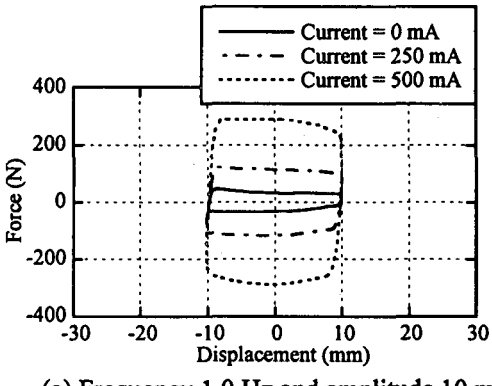

(a) Frequency 1.0 Hz and amplitude 10 mm

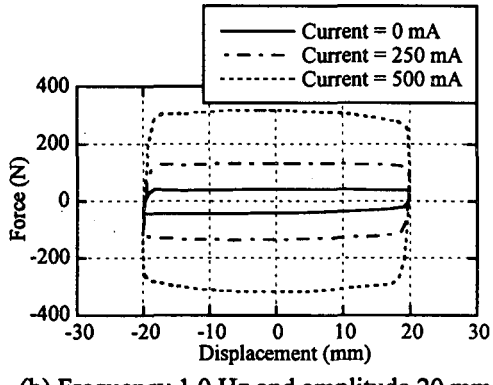

(b) Frequency 1.0 Hz and amplitude 20 mm

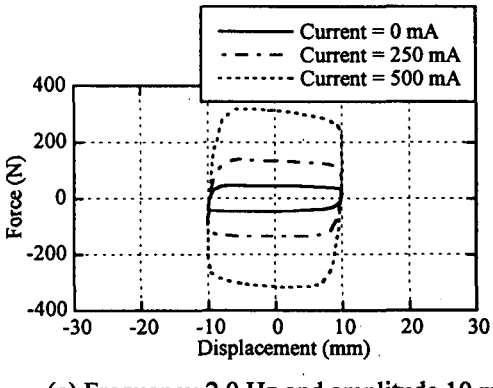

(c) Frequency 2.0 Hz and amplitude 10 mm

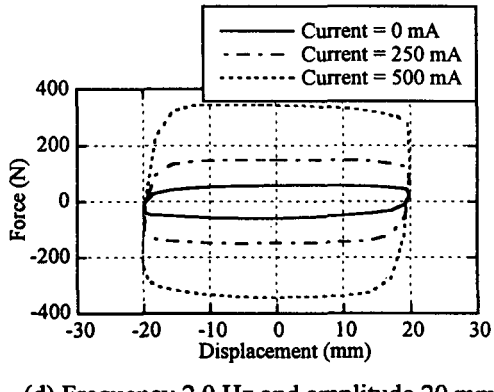

(d) Frequency 2.0 Hz and amplitude 20 mm

Fig. 4 Response of MR damper subjected to various loading conditions

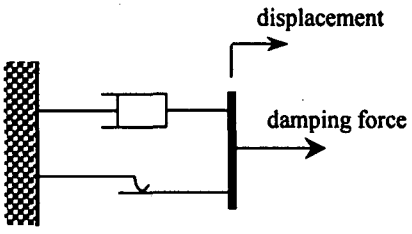

Fig. 5 Bingham model of MR damper

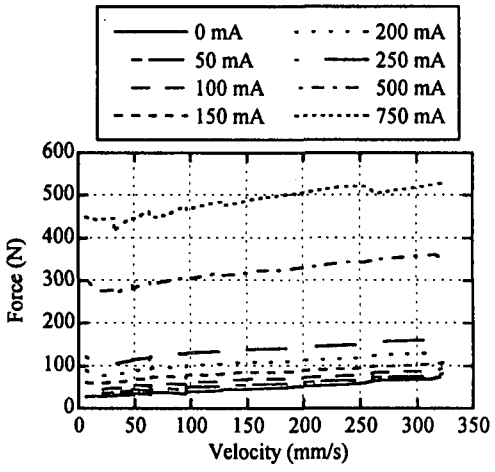

Fig. 6 maximum force-velocity relationship

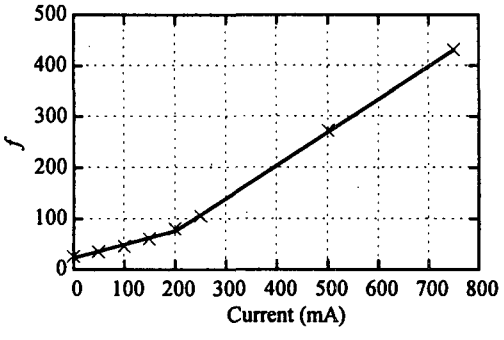

(a) f vs. current

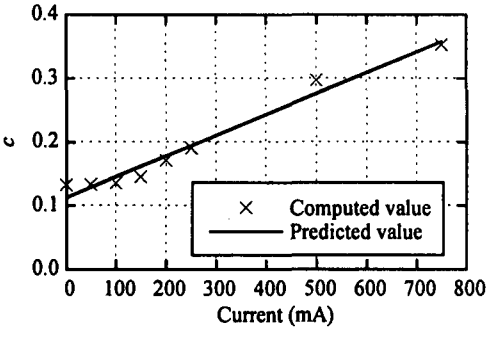

(b) c vs. current

Fig. 7 Parameters f and c from regression analysis

velocity are determined and shown in Fig. 6 of various current levels. It is found that for a particular current, the damping force varies quite linearly with the velocity. And as the current increases, the damping force increases while the dependency of the damping force on the velocity does not significantly change. From regression analysis, the damping force for each current level is modeled by Eq. (1). And because f and c varies with the current, the dependencies of f and c on the current are expressed as

$$f=\begin{cases} 22.6+0.267\times current & ; \quad current<200mA \\ -53.4+0.647\times current & ; \quad current>200mA \end{cases} \quad (2)$$

$$c=0.113+0.000327\times current \quad (3)$$

Fig. 7 shows the comparison of the parameters f and c determined from the regression analysis of the experimental results and those determined from Eqs. (2) and (3). The damping force predicted by Eqs. (1)- (3) is illustrated in Fig. 8. Comparing Fig. 6 to Fig. 8, it is seen that the damping force can be predicted by Eqs. (1)-(3) with good accuracy.

4. MR DAMPER UNDER FLUCTUATING CURRENT

The model of the MR damper was developed based on the cyclic loading test for constant current levels. In actual control application, the damper is subjected to fluctuating current depending on structural response. Consequently, the characteristic of the damper under fluctuating current needs to be investigated.

When a current is suddenly applied to the damper, time is required for MR fluid to reach its rheological equilibrium. Referring to Fig. 9, when a square current with a time interval and current level is supplied to the damper, the damping force increases and then becomes constant. The rising time t_r is defined as the duration from the time of applying the current to the time that the damping force becomes constant. And when the current is terminated, the damping force decreases and then becomes constant. The falling time t_f is defined as the duration from the time of terminating the current to the time that the damping force becomes constant.

To determine the rising and falling time, a cyclic loading test is conducted for square current with

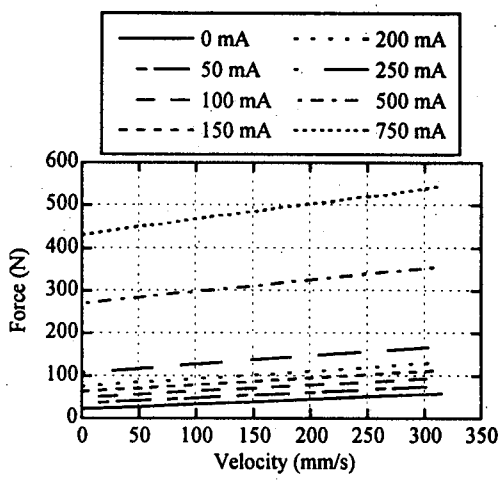

Fig. 8 maximum force-velocity relationship by Eqs. (1)-(3)

various time intervals and current levels. Fig. 10 shows time histories of damping force measured from the experiment and that predicted from Eqs. (1)-(3) for a 0.5 Hz sinusoid with an amplitude of 20 mm. It is seen that for time interval of 40 ms, the damping force cannot reach the predicted damping force, but when the longer time interval of applied current is provided, the measured and predicted damping forces are almost the same. The predicted and measured differential forces are represented by a force ratio R_f defined as

$$R_f = \frac{\Delta f_{d,measured}}{\Delta f_{d,predicted}} \tag{4}$$

where $\Delta f_{d,measured}$ is a measured differential damping force and $\Delta f_{d,predicted}$ is a predicted differential damping force. Fig. 11 shows the force ratio versus time interval of applied current. It is seen that the force ratio comes close to 1.0 when the time interval is larger than 140 ms. So, the rising time is considered as 140 ms. Fig. 12 shows the differential damping force versus falling time. The falling time increases with the differential force at the termination of current. It is worthy to note that the rising time and falling time would limit the accuracy of the application of the model to control the MR damper to some extent.

5. CONTROL ALGORITHM AND EXPERIMENT VERIFICATION

This study investigates two control algorithms that preset the relationship between damping force and displacement or velocity. The purpose of the control algorithms is to dissipate energy and to break relative movement between two structures connected by the MR damper in order to prevent pounding or unseating.

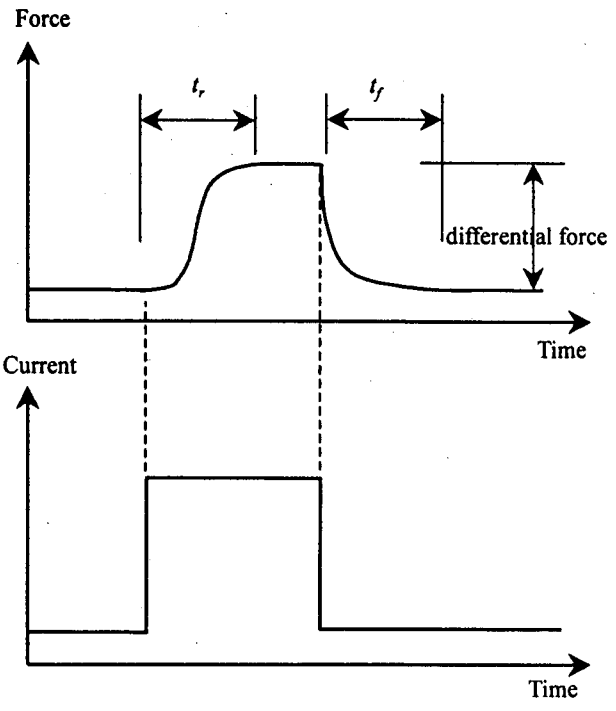

Fig. 9 Definition of rising time and falling time

Fig. 13 shows Algorithm 1 that damping force is commanded as a function of displacement. When absolute displacement is less than d_1, the damping force is set equal to f_1 that mainly functions to dissipate energy. And when absolute displacement exceeds d_1, damping force is commanded to increase linearly to f_2 at d_2. The increase of damping force is intended to break the further movement. Fig. 14 illustrates Algorithm 2 that the damping coefficient is varied with displacement and velocity of the damper. When displacement and velocity have the same sign, meaning that two structures connected by the damper are approaching or moving apart each other, the damping coefficient is set to a large value c_1. But when displacement and velocity have the opposite sign, the damping coefficient is set to a small value c_2.

To study the extent to which the control algorithms can be implemented by the MR damper, a series of cyclic loading tests is performed. By applying the model of the MR damper, the control of damping force according to the control algorithm can be made. Fig. 15 and Fig. 16 show the comparison between the commanded force and measured force for various loading frequencies for Algorithms 1 and 2, respectively. It is found that the damping force can be produced according to the control algorithms. However, some discrepancies of damping force are observed, especially when the damping force is abruptly changed. And as loading frequency increases, the discrepancy increases. The limited accuracy is due to the response time of the MR damper as mentioned above. For further

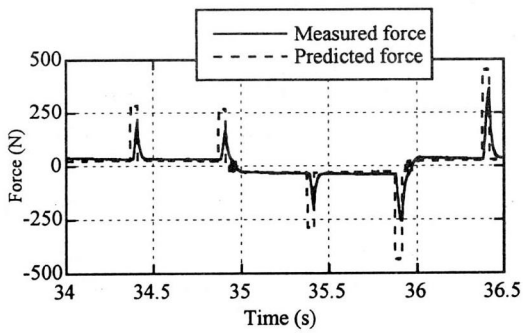

(a) time interval = 40 ms

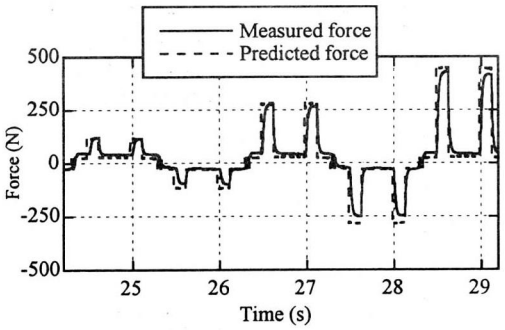

(b) time interval = 140 ms

Fig. 10 Comparison of predicted and measured damping force

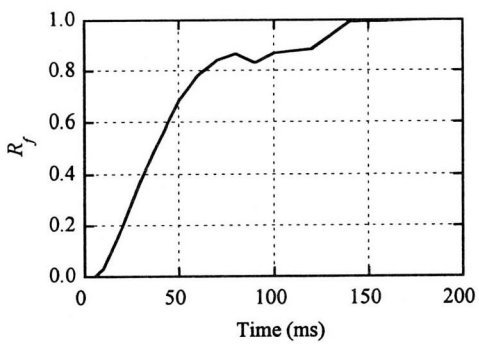

Fig. 11 R_f vs. time interval

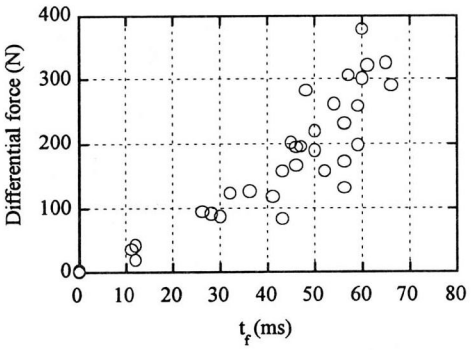

Fig. 12 Damping force vs. falling time

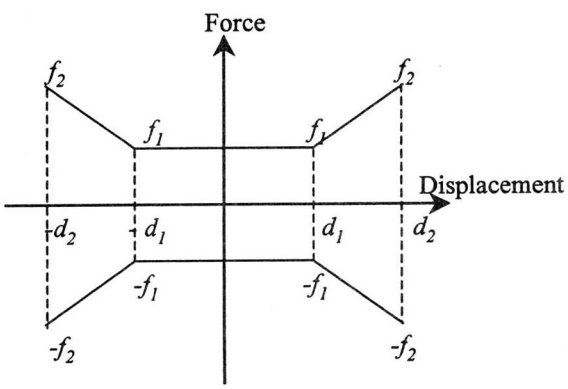

Fig. 13 Algorithm 1

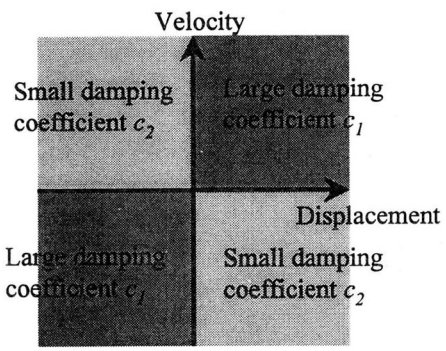

Fig. 14 Algorithm 2

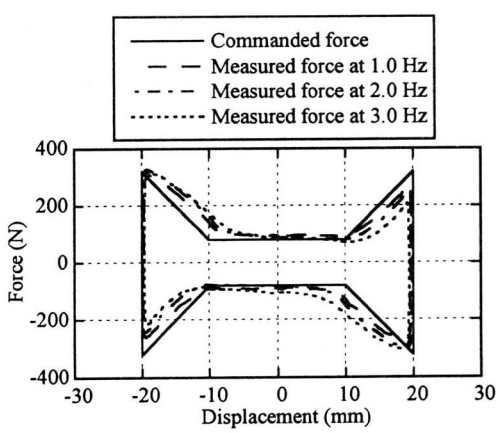

Fig. 15 Comparison of the commanded and measured force for algorithm 1

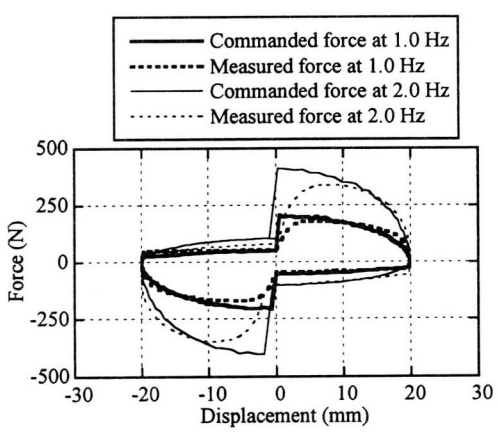

Fig. 16 Comparison of the commanded and measured force for algorithm 2

investigation, it is necessary to improve the control of the damping force by taking into account the effect of rising and falling time of the MR damper.

6. CONCLUSIONS

The study on application of a MR damper for semi-active control of bridges is conducted experimentally by a series of cyclic loading tests. From the investigation, it can be concluded that:

1) From the results of cyclic loading test of the MR damper for various loading conditions and current levels, it is found that damping force depends on input current levels and velocity. The MR damper can be modeled by the Bingham model consisting of friction and viscous elements with good accuracy.

2) In actual application, the MR damper is subjected to fluctuating current. The accuracy of the model is limited by the time required for MR fluid to reach its rheological equilibrium. Consequently, further investigation is necessary to improve the control of damping force by taking into account such an effect.

3) The damping force is commanded according to two control algorithms that vary damping force with displacement or velocity. It is found that damping force can be generated according to the control algorithms. However, some discrepancies are observed when the damping force is abruptly changed and the loading frequency increases.

ACKNOWLEDGEMENTS: The MR damper used in this study is provided by Sanwa Tekki Corporation. The authors appreciate Dr. Katsuaki Sunakoda and Hiroshi Sodeyama for their kind cooperation. The authors are thankful to Professor Billie F. Spencer, University of Notre Dame for his constructive comment. Special thanks are due to Gaku Shoji, Gakuho Watanabe, and Kenji Uehara for contribution in conducting cyclic loading test.

REFERENCES

1) Symans, M. D. and Constantinou, M. C., Semi-Active Control Systems for Seismic Protection of Structures: a State-of-the-Art Review, *Engineering Structures*, 21, pp. 469-487, 1999.
2) Kawashima, K. and Unjoh, S., Seismic Response Control of Bridges by Variable Dampers, *Journal of Structural Engineering, ASCE*, 120-9, pp. 2583-2601, 1994.
3) Spencer, B. F., Dyke, S. J., Sain, M. K., and Carlson, J. D., Phenomenological Model of a Magnetorheological Damper, *Journal of Engineering Mechanics, ASCE*, 123-3, pp. 230-238, 1997.
4) Jolly, M. R., Bender, J. W., and Carlson, J. D., Properties and Applications of Commercial Magnetorheological Fluids, *SPIE 5th Annual Int. Symposium on Smart Structures and Materials*, San Diego, USA, 1998.
5) Sunakoda, K., Sodeyama, H., Iwata, N., Fujitani, H., and Soda, S., Dynamic Characteristics of Magneto-Rheological Fluid Damper, *SPIE 7th Annual Int. Symposium on Smart Structures and Materials*, Newport Beach, USA, 2000.